

# Quantifying tectonic versus erosive denudation by the sediment budget: the Miocene core complexes of the Alps

J. Kuhlemann\*, W. Frisch, I. Dunkl, B. Székely

*Institut für Geologie und Paläontologie, Universität Tübingen, Sigwartstrasse 10, D-72076 Tübingen, Germany*

Received 15 March 2000; accepted 16 August 2000

## Abstract

The denudation budget of the Alps is quantified for the main period of lateral extrusion between 22 and 12 Ma. The relative importance of tectonic denudation increases from W to E from ~70% in the Lepontine window in the Swiss Alps to ~80% in the Tauern window and to more than 95% in the Rechnitz window. The driving mechanism of tectonic denudation was eastward extrusion due to an unconstrained orogenic margin in the Pannonian basin. Tectonic denudation in the Alps was responsible for about 30% of the total exhumation between 22 and 12 Ma. © 2001 Elsevier Science B.V. All rights reserved.

*Keywords:* Alps; core complex; sediment budget; erosion rates; exhumation rates; tectonic denudation

## 1. Introduction

Tectonic denudation and fast exhumation of foot-wall rock in excess of 1 mm/yr is found in several tectonic settings. Core complexes situated in young collisional orogens often form high mountain ranges due to pre- and synextensional crustal thickening, isostatic uplift and erosion (e.g. Tucker and Slingerland, 1996). Both maximum crustal thickness and highest relief are typically located along the axis of Alpine-type collisional orogens. A thick, thermally softened crust and an orogen-parallel topographic gradient represent preconditions for gravitational instability, which induces orogenic collapse and exhumation of metamorphic domes (e.g. Wernicke, 1981). The Eastern Alps (Fig. 1) provide a classical example for lateral extrusion towards an unconstrained margin (Ratschbacher et al., 1991a,b).

Exhumation of rock means the approaching of a rock particle to the Earth's surface (England and Molnar 1990), which is, e.g. recorded by cooling rates calculated from thermochronologic data (e.g. Foster and John, 1999). The commonly used closure temperature concept for thermochronologic cooling ages needs reasonable assumptions for the paleo-geothermal gradient to model rates of exhumation (Grasemann and Mancktelow, 1993; Mancktelow and Grasemann, 1997).

Exhumation of deeply seated rocks can be enabled (Fig. 2) both by surface erosion and tectonic denudation. The latter process laterally removes hanging-wall rock along low-angle detachment faults.

Tectonic denudation can potentially exhume rocks from great depths under constant cover of synrift and postrift sediments, e.g. as in the Pannonian basin (Tari et al., 1999), or by creating only a minor topography, e.g. as in parts of the Aegean region (Lister et al., 1984). In such cases, surface erosion is obviously not or not a relevant factor of exhumation.

\* Corresponding author. Fax: +49-7071-5059.

*E-mail address:* kuhlemann@uni-tuebingen.de (J. Kuhlemann).

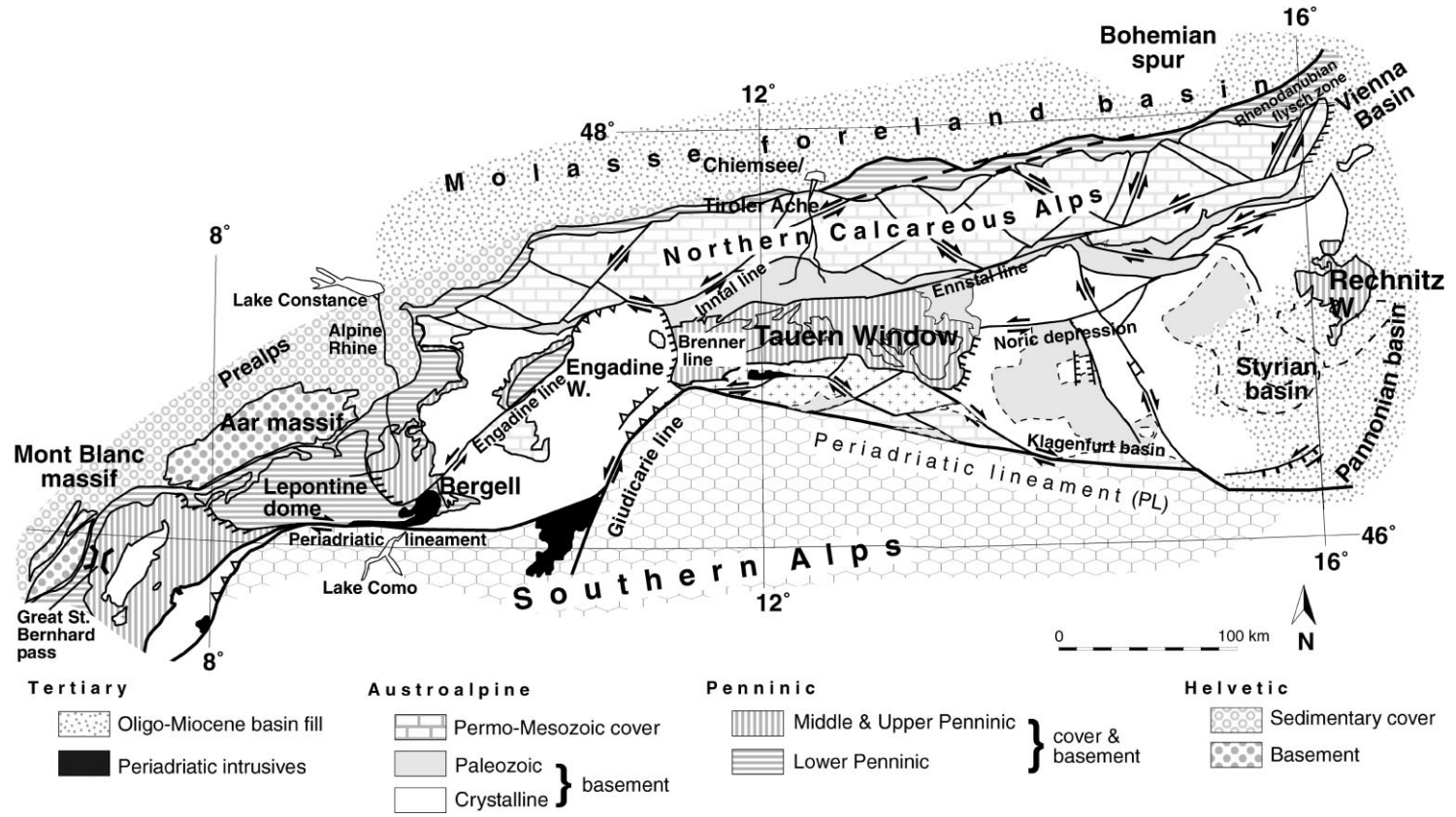


Fig. 1. Structural sketch map of the Swiss and Eastern Alps. In this paper, we use the meridian of the Alpine Rhine river to separate the area of the Eastern Alps from the Swiss and Western Alps, respectively.

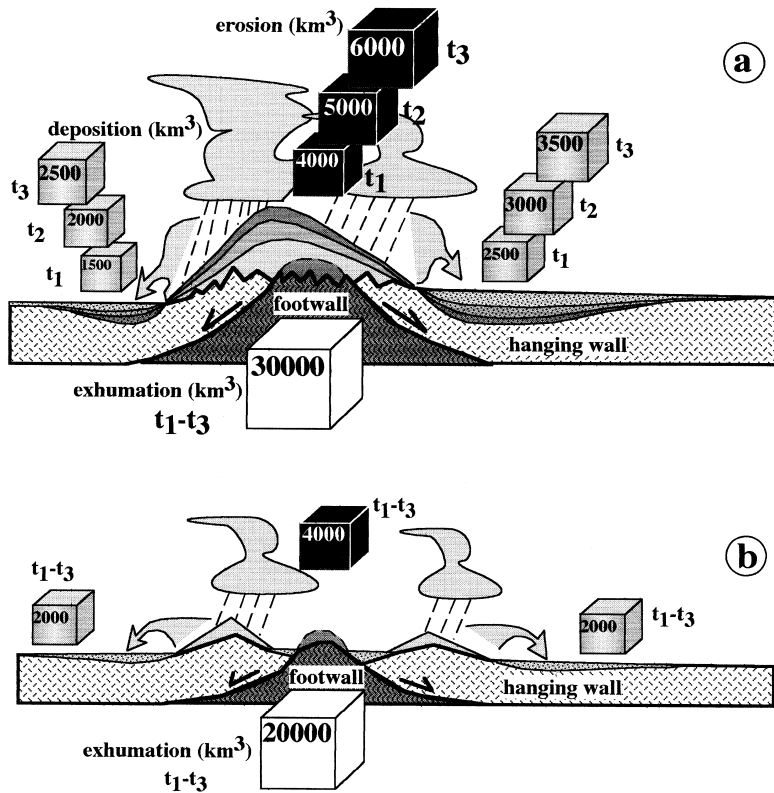


Fig. 2. Cartoon of the basic principle of the sediment budget method, indicating (a) eroded and deposited rock volumes according to time slices ( $t_1$ – $t_3$ ). In scenario (a) exhumation of a metamorphic core complex in an evolving mountain chain is performed both by erosion and tectonic denudation (50/50%). The footwall is first exposed during erosion period  $t_3$ . In scenario (b), drawn only for time slice  $t_3$ , the exposed footwall is largely buried by syntectonic debris, derived from both the hanging wall and the footwall. Surface erosion contributes only 20% to the exhumation of the footwall rock.

Contrasting to this, Miocene core complexes like Muztag Ata and Kongur Shan, lined up along the Karakoram fault in central Asia (Brunel et al., 1994), display heavily glaciated, vast dome-shaped morphoforms with the highest peak elevations in the region (>7000 m). In these two cases, and similar examples of high relief, the contribution of surface erosion to the overall exhumation maybe a relevant factor but its relative amount remains unknown. Surface erosion has the principle potential to exhume rocks from deep structural levels, since erosion rates of several mm/yr are observed, e.g. in New Zealand and Taiwan (Milliman and Syvitski, 1992), and the eastern Himalayan syntaxis (Burg et al., 1997).

One possible approximation to assess the contribution of erosion to exhumation of a core complex is to

investigate cooling rates of hanging wall-rocks from its structural frame. Since the hanging wall-rocks may be heated by the exhuming footwall of the evolving core complex, heat flow-modelling is needed to roughly convert cooling rates into erosion rates (Grasemann and Mancktelow, 1993; Dunkl et al., 1998). Further uncertainty originates from potentially different erodibility of footwall and hanging wall rock, which will depend on lithology, degree of deformation, and alteration of rock by fluids.

A second method to detect tectonic exhumation are thermochronological studies of detrital grains and pebbles in subsequently generated debris (e.g. Brandon and Vance, 1992; Brügel et al., 2000; Dunkl et al., 2000b). During moderate erosional unroofing in crystalline source terrains cooling ages

of the orogenic debris should record continuous younging with decreasing age of sedimentation, and with cooling ages being several My (tens of My) older than the age of sedimentation (e.g. Brandon and Vance, 1992). A sudden appearance of cooling ages close to sedimentation age (e.g. a few My) indicates a sudden exposure of tectonically unroofed footwall rock (Frisch et al., 1999). In the latter case, rocks with the missing cooling age spectrum have not been eroded but are still preserved in the deeper parts of the hanging-wall unit, which were laterally removed from the core complex by tectonic denudation (Frisch et al., 1999). However, this method suffers of similar problems with the paleo-geothermal gradient in the structural frame of a core complex as thermochronologic studies of the source terrain itself.

A third method is a tectonic reconstruction, which uses thermochronological data to detect the boundaries of the core complex (Frisch et al., 1998). Geometric constraints are used to set up a budget of crustal shortening, thickening, and lateral extension. Approximate rates of lateral extension and the geometry of low-angle detachment faults enable to deduce the amount of tectonic denudation (see Frisch et al., 2000a).

### *1.1. A supplementary strategy: the sediment budget method*

The method applied here is to quantify the sediment budget of the orogen during periods of accelerated exhumation of rocks from deeper crustal levels. The advantage of the sediment budget record is its direct monitoring of surface erosion. The mass of sediments allows a calculation of average erosion rates of the source terrain (Fig. 2; e.g. Einsele et al., 1996). If the exhumation of deeper crustal levels in a tectonic window requires the removal of considerably more hanging wall-rock than is present in the solid rock volume of the time-equivalent sediments, tectonic denudation should have contributed to the process of exhumation. The volume of these sediments will also include a contribution from the mountainous source terrains surrounding the core complex. The more debris derives from the frame of the tectonic window, the less is contributed from the hanging wall of the exhuming core complex, and thus the more important the process of tectonic denudation should have been (see Fig. 2).

The disadvantage of the sediment budget method is its poor spatial resolution. Even if debris of source terrains in the near vicinity of core complexes can be identified by means of petrographic composition of gravel and sand, fine-grained deposits in further distance and in particular the dissolved load can hardly be traced back to the source terrains. Unfortunately, silty and clayey debris forms the major mass of circum-Alpine deposits, and may contribute around 85% of the total load (e.g. Einsele and Hinderer, 1997; Mangelsdorf, 1977; Fig. 3).

In this paper we use the sediment budget and published thermochronological data to quantify the contribution of both erosional and tectonic denudation for the exhumation of the most important core complexes of the Alps. The Tauern window, a classic Alpine example of a core complex with a high relief, is treated in more detail.

## **2. Method and error estimate**

The sediment budget of the Alps is set up by the calculation of sediment volumes of all circum-Alpine basins, based on literature. This has been performed by digitizing all available thickness maps of strata and base contour lines of sedimentary basins, as well as planimetry of geological profiles. The calculated volumes of sediment were then recomputed to a porosity equivalent to the solid rock of the source terrain. If density data of the sedimentary basin fill was not available, it was calculated on the base of porosity data and seismic velocities. If such data were also lacking, the standard compaction curves of Daly et al. (1966), plus an additional 7% compaction due to the presence of ductily behaving grains (see Pittman and Larese, 1991), were applied. These steps of calculation were performed within a potential error range of about  $\pm 10\%$  each. This error estimate is based on several repetitions of the calculation procedure, using independent data sources for the same basin. The base data are discussed in detail by Kuhlemann (2000). The solid rock-equivalent sediment volumes of the basins were separated into formations of known stratigraphic age to achieve the best possible time resolution. A resolution of 0.5 and 1 My time steps is chosen for the Eastern Alps (Fig. 4), and for the Swiss and Western Alps, respectively, as the

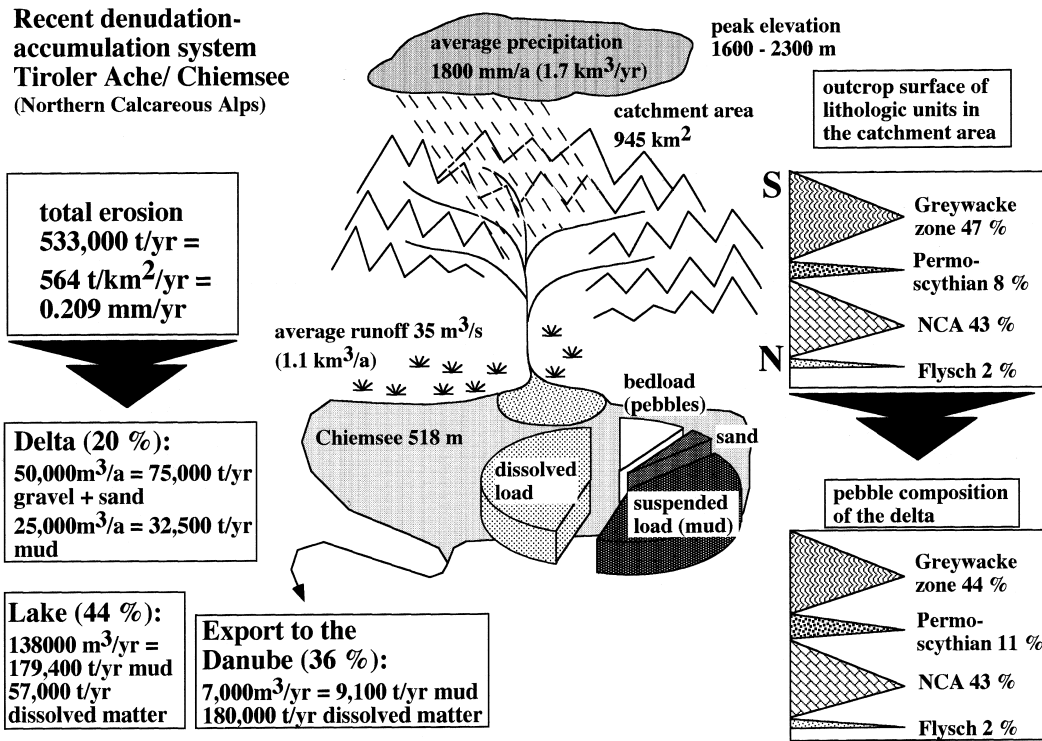


Fig. 3. Recent sediment budget of the Tiroler Ache with differentiated volumes of bedload, suspended and dissolved load (in%, center), and loci and mass of deposition of debris (left side and bottom center; Mangelsdorf, 1977). The lithotype proportions in the pebble spectrum (small pebbles of 2–5 cm included) of the Tiroler Ache on the right side (Skeries and Troll, 1991) grossly reflect the area covered by these rocks, despite of the contrasting resistivity of the pebbles.

shortest recognizable stratigraphic unit for East Alpine sediments is 0.8 My long and enables a higher time resolution than for Swiss and Western Alpine sediments. Although a high-resolution magnetostratigraphy is available for the Swiss molasse (Schlunegger et al., 1996; Kempf et al., 1997; Kempf and Matter, 1999), the isochrons are not yet established basinwide.

This transformation from a stratigraphic relative age to chronostratigraphic time scales represents a severe source of error (Fig. 5). Comparing ages attributed to stratigraphic boundaries during the last 10 years (Fig. 6, with references) a high divergence in the age estimates is evident. With respect to the most commonly used stratigraphic time tables we refer to the chronostratigraphic charts of Berggren et al. (1995), Steininger et al. (1996) and Rögl (1996). Alternative time calibrations are provided by regional studies, such as Kempf et al. (1999).

The second severe source of error is related to the

fact that most basins are not supplied exclusively from the Alps but also from other source terrains. This is a particular complication for late Miocene to recent sediments. It is a minor problem as long as the basin is situated relatively close to the Alps, which represent the major source. In such cases the potential error is typically in the range of  $\pm 20\%$ , since the available provenance data (e.g. heavy mineral and pebble lithology composition) often allow a clear separation of different sources for each formation. In the case of a shallow marine or even tidally influenced environment, the potential error rises significantly due to mixing of fine grained debris (see also Schlunegger, 1999). In this case, the separation of sources is based on the relative amount of key minerals from the marine sediment, and the end-member heavy mineral composition prior to and after the marine phase.

As the catchment size of the basin increases with increasing distance from the Alps, their relative

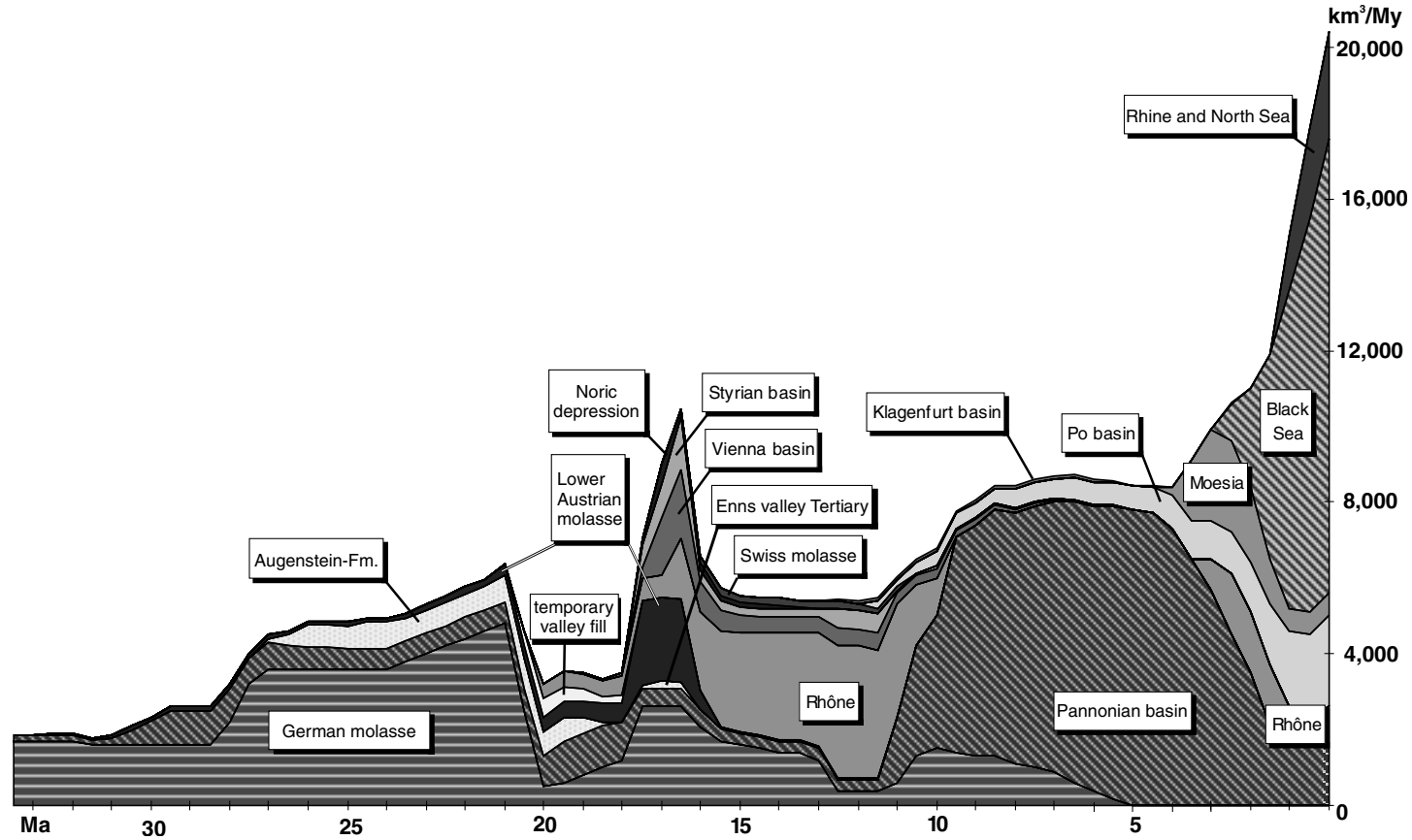


Fig. 4. Volume of sediment derived from the Eastern Alps (sediment discharge rates in  $\text{km}^3/\text{My}$  of solid rock of  $\delta = 2.7 \text{ g/cm}^3$ ), separated for the basins involved. Molasse deposits on top of the Northern Calcareous Alps are termed 'Augenstein-Fm'. Temporary valley fill occurred due to rapid subsidence during the establishment of the Burdigalian seaway in the foreland basin. Export to the Rhône fan occurred during overfilling of the foreland basin (Upper Freshwater Molasse) and in Plio-Pleistocene times, when the headwaters of the modern Alpine Rhine were tributary to the Rhône. Overfilling of the Pannonian basin in Plio-Pleistocene times resulted in deposition on the Moesian platform along the course of the Danube to the Black Sea. A south-directed drainage pattern developed after 12 Ma in the southwestern part of the Eastern Alps (Brügel, 1998).

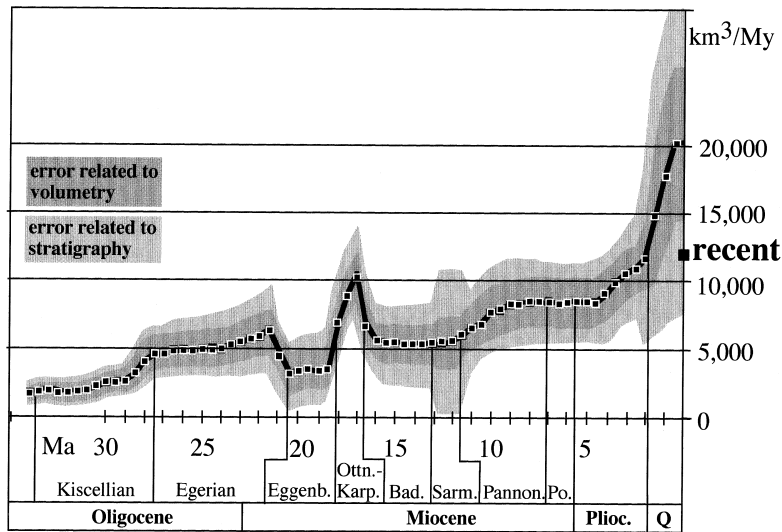


Fig. 5.  $1\sigma$  error bar envelope of the East Alpine sediment discharge rates ( $\text{km}^3/\text{My}$ ), calculated from the error range of volume estimates and the error range of chronostratigraphic ages (see Fig. 6). The 'recent' sediment discharge rate is calculated from river load data which is calibrated (expanded) according to delta growth rates (Kuhlemann, 2000).

contribution of debris to the basin fill will decrease and may give rise to an unacceptably high error. In this case, only the budget of local and regional Alpine semi-enclosed lake systems (temporal scale of 10–10,000 years) and the evaluation of large catchments with multiple sources allows the error to be limited. This actualistic approach has to be applied in the case of the Pleistocene Rhine catchment and the late Pliocene–Pleistocene Danube catchment (see Einsele and Hinderer, 1997; Kuhlemann, 2000). The error is estimated to be in the range of  $\pm 30\%$ .

The export and diffuse spread of dissolved material had to be estimated in several cases. The relative amount of dissolved load as compared to the solid load, represented by suspended load and bedload, is related to the areal extent of key lithologies such as carbonates, feldspar-rich basement rocks and quartzites. The areal distribution of these lithologies in the geological past is reconstructed from the record in the foreland fans (e.g. Schiemenz, 1960), which has been compiled in maps (e.g. Frisch et al., 1998; Schlunegger, 1999). Such key lithologies produce a characteristic relative amount of dissolved load, which has been extracted from recent river load measurements (e.g. Sommer, 1980; Schröder and Theune, 1984). For the recent setting of the Alps

with a number of river load data, the error for the bulk amount of dissolved load of these rivers is estimated in the range of  $\pm 30\%$ . The relative amount of dissolved load is influenced by the intensity of chemical weathering and thus by the climate, and can be estimated only very roughly. The potential error for estimates of the exported dissolved load may reach up to  $\pm 50\%$ .

Redeposition is a major problem in the subalpine molasse, since the restoration of imbricated molasse thrust sheets (e.g. Pfiffner, 1986) is an important source of error (see Schlunegger et al., 1997). In the North Alpine foreland basin this potential error effects mainly the Oligocene and early Miocene sediment budget, whereas the South Alpine foreland basin suffered massive reworking in middle Miocene times (Schönborn, 1992) and latest Miocene times (Messinian; e.g. Ryan and Cita, 1978). Moreover, during thrusting of imbricated subalpine molasse the amount of immediate ( $<1$  My) redeposition is difficult to estimate.

In the face of these variable and sometimes potentially high errors, any well-founded interpretation seems to be impossible, and even drastic changes of erosion rates may not be statistically substantiated within conventional confidence levels of 90 or 95% ( $2\sigma$  error). Although this fact cannot be neglected, a

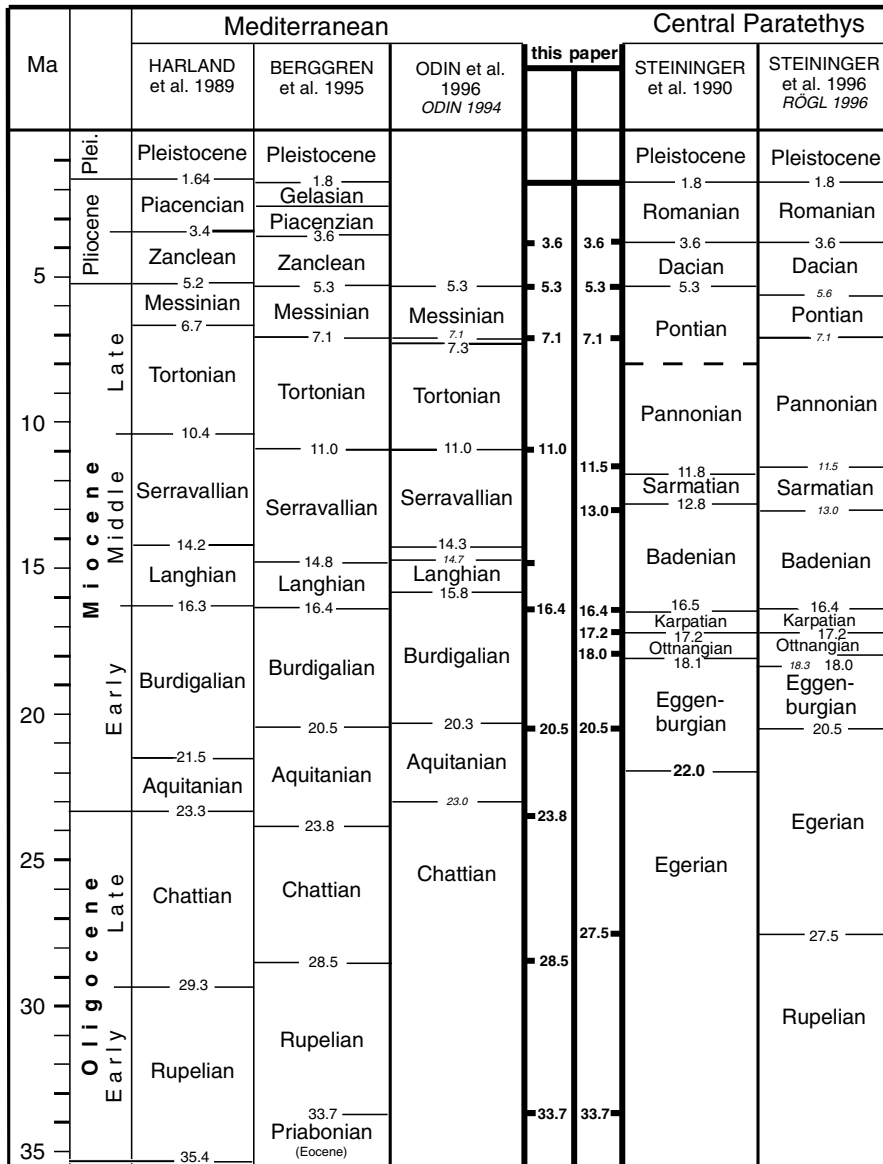


Fig. 6. Chronostratigraphic correlation chart, comparing chronostratigraphic age determinations after 1989. Both Mediterranean and Paratethys time scales have been applied to compute chronostratigraphic ages to formations in the basins addressed in Fig. 4. Sources: Harland et al., 1989, Steininger et al. (1990, 1996). Odin (1994), Odin et al. (1996), Berggren et al. (1995), Rögl (1996).

geological explanation of the sediment budget curve is still meaningful for the following reasons:

(1) The addition of several maximum potential errors is unlikely. Multiple potential errors are expected not to develop in a single direction but tend to partly compensate each other. Certainly it

remains unknown just how strongly a possible overestimate in one step of calculation may be compensated by an underestimate in another step of calculation.

(2) A statistical evaluation of the propagation of potential errors estimated for separate basins and

formations of the Eastern Alps (see Bevington, 1969; Appendix A) reveals that, at a confidence level of 65% ( $1\sigma$  error), major calculated changes of erosion rates and thus the reconstructed general trend are significant. In our statistical approach, we suppose that the data derived from different sources are realizations of statistical variables. This is only partly true because these data mostly represent computed values of measurements. The second assumption is that the 'raw data' are independent. In many cases, namely if the basins are situated far from each other or formed at different times, this assumption is reasonable. In other cases, such as the Pannonian basin, the Moesian platform and the Black Sea, this assumption is not valid, especially during overfilling of the Pannonian basin in Plio-Pleistocene times. On the other hand, the coupling is not too strong since these basins were supplied by other source terrains, which increases the independency of the basins from each other and thus the statistical behaviour of the data set. The potential effect of coupling is taken into account partially in another way, in that the errors of the individual data points were slightly overestimated.

Having kept in mind the limited validity of these two assumptions, a relative estimated error percentage for each individual sedimentary basin and each time interval (0.5 My) has been assigned. The relative errors range from 20 to as high as 100%, while 50% is the typical value (Table A1, appendix). The absolute errors are now calculated from the relative ones, and square-summed for the contributing basins to get the variance for each individual time step (Fig. 5). This type of error estimation contains only the errors from the volumetry, but does not contain the possible effect of the erroneous length of stratigraphic units in the geological time table, erroneous stratigraphic age determination of formations, and an error related to an artificially high stratigraphic resolution of 0.5 My. To estimate the error of the length of stratigraphic units, the variability is treated as a typical error range except for the periods shorter than 2 My, where the small variability reflects lack of independent data rather than anomalously high precision. In these cases, an error of up to  $\pm 40\%$  results. Erroneous stratigraphic age determination of formations range around  $\pm 20\%$  in pre-Pleistocene times and about 40% for the Pleistocene, referring to Fig. 3. Since the timespan is in the denominator for the calculation, the relative

errors are additive increasing the overall error of the volume calculation.

### 3. Geodynamic setting of the Alps in Miocene times

The Alps are analysed in great detail by means of thermochronological (e.g. Frank et al., 1987; Hunziker et al., 1992; Hunziker et al., 1997) and structural methods (e.g. Ratschbacher et al., 1991b; Schmid et al., 1997). The kinematics of Alpine metamorphic core complexes during exhumation are characterized by large-scale E–W extension (Steck and Hunziker 1994; Frisch et al., 2000a) and ductile detachment shear zones at the base of the hanging wall (Selverstone, 1988; Mancktelow, 1985).

Within the Eastern Alps three tectonic windows are known, of which the Tauern window is the largest one (see Fig. 1). A fast exhumation of the Tauern window is recorded from about 22 until about 13 Ma by several geochronometers (Cliff et al., 1985; Frank et al., 1987; Blanckenburg et al., 1989; Fügenschuh et al., 1997; Dunkl et al., 2000a). It has been related to the process of lateral extrusion (Ratschbacher et al., 1991a), starting at about 22 Ma in the eastern parts of the Tauern window (Fig. 7) and ending at about 13–12 Ma (Frisch et al., 1999). During the time of lateral extrusion a 15–20 km, in average possibly

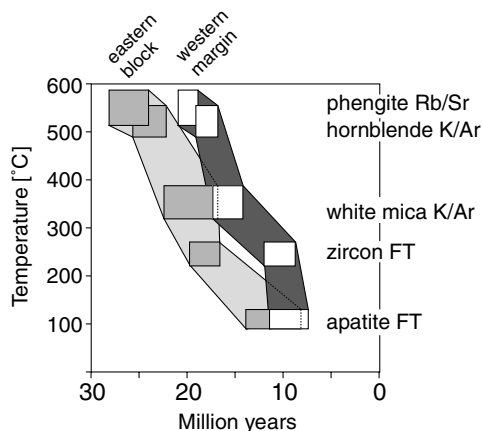


Fig. 7. Temperature–time plot of the thermochronologic data from the western and eastern part of the Tauern Window. Data from western margin: Fügenschuh et al. (1997), Blanckenburg et al. (1989); data from the eastern part of the window: Cliff et al. (1985), Oxburgh et al. (1966), Reddy et al. (1993) and Dunkl et al. (2000b).

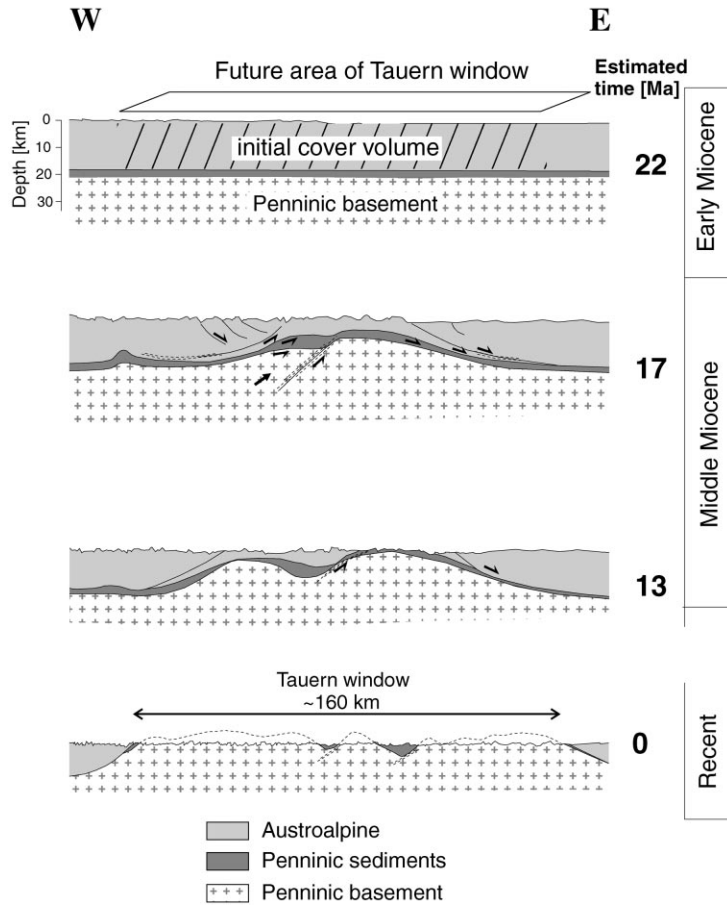


Fig. 8. Kinematic evolution of unroofing of the Penninic footwall of the Tauern window along the central E–W profile, simplified after Frisch et al. (in press a).

16 km thick pile of hanging wall (Blanckenburg et al., 1989) was removed from the 5000 km<sup>2</sup> area of the Tauern window (Fig. 8).

The Lower Engadine window in the western Eastern Alps covers 1000 km<sup>2</sup> and extends along the sinistral Engadine fault, which was active around the Oligocene–Miocene boundary (Schmid and Froitzheim, 1993) and has probably exhumed Penninic substratum within a pull-apart geometry (Waibel and Frisch, 1989). In this window only the higher parts of the Penninic units are exposed. Due to the relatively small size, lack of fission track cooling ages, and the early time of extension this case is not discussed in detail.

The Rechnitz window is situated in the eastern

margin of the Eastern Alps. It is only about 500 km<sup>2</sup> large and partly buried by sediments of Miocene age. The exhumation of the footwall rock culminated between 19 and 14 Ma (Ratschbacher et al., 1990; Dunkl and Demény, 1997; Dunkl et al., 1998).

The Lepontine dome in the Swiss Alps covers an area of about 3500 km<sup>2</sup>, and has been rapidly exhumed from depths of about 15–20 km between about 22 and 17 Ma (Hunziker et al., 1992), possibly already starting at 25 Ma (Schlunegger and Willett, 1999), but fast exhumation continued at least until 11 Ma in the westernmost parts (Bradbury and Nolen-Hoeksema, 1985; Grasmann and Mancktelow, 1993; Hunziker et al., 1997). In contrast to the Tauern and Rechnitz windows, the main detachment

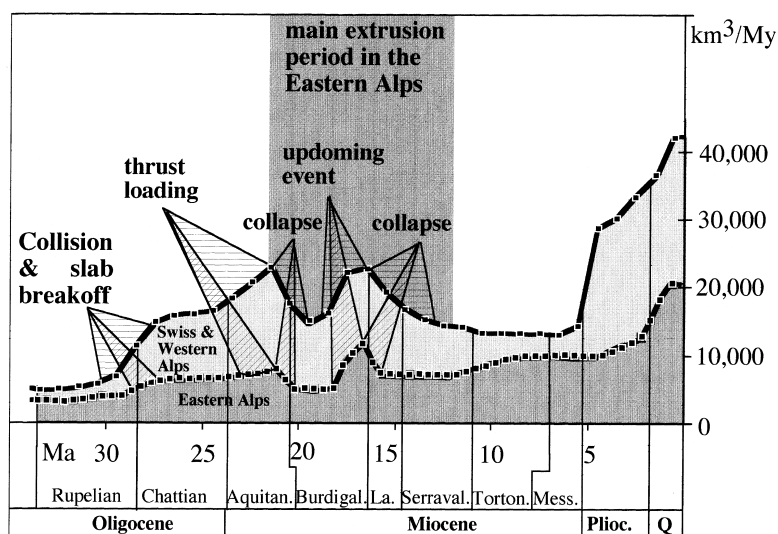


Fig. 9. Controlling factors of sediment discharge from the Alps between 24 and 10 Ma.

fault is not situated at the Austroalpine–Penninic boundary but within the Penninic nappe stack (Steck and Hunziker, 1994).

#### 4. Post-collisional sediment budget history of the Alps

##### 4.1. The 30 Ma event

The post-collisional erosion history of the Alps is starting with an uplift event around 30–28 Ma, when the sediment accumulation rates were doubled (Fig. 9) and the foreland basin setting changed from the under-filled flysch stage to the molasse stage (Sinclair, 1997). This increase of sediment accumulation is explained by the continental collision (see, e.g. Willett et al., 1993) and slab breakoff sensu Blanckenburg and Davies (1995), with a decoupling of the dense and heavy lithospheric slab, subsequent uplift and increasing relief. Note that the sediment discharge did not decrease after a short-lived thermal event related to Periadriatic magmatic activity, but reached steady state after a response time of 2–3 Ma.

##### 4.2. The Aquitanian phase

The Miocene sediment budget of the Swiss and Western and, less strongly expressed, also of the East-

ern Alps shows an increase between 24 and 21 Ma (Fig. 9). It is related to the buildup of topography and relief in the Swiss and Western Alps and the westernmost Eastern Alps (Frisch et al., 1998), whereas surface erosion and probably also relief in the eastern Eastern Alps declined (Reinecker, 2000). An increase of relief in the western and central parts of the Alps is recorded by a strong increase of the pebble size in the foreland fans (e.g. Schiemenz, 1960). The increasing topographic gradient towards the E, enhancing the gravitational instability, provided a precondition for lateral extrusion (Frisch et al., 1998, 2000a).

##### 4.3. The 21 Ma event

At 21 Ma the sediment discharge rates of the entire Alps dropped dramatically (Fig. 9; Kuhlemann et al., 2000). This event occurred coeval with the reduction of thrust advance rates in the Swiss Molasse zone to at least one third (Homewood et al., 1986). In the easternmost part of the orogen, thrusting continued until ~17 Ma (Decker and Peresson, 1996). From 21 Ma on, for about 9 My, an important part of the plate convergence was compensated by extension, extrusion and tectonic escape (Ratschbacher et al., 1991a). This was driven by gravity from the highly elevated parts of the Alps towards the E, and

indentation of the South Alpine block, together exhuming the footwall of the Austroalpine lid (Frisch et al., 2000a). Some minor E–W extension prior to this event may have occurred (Schlunegger and Willert, 1999).

The reduction of foreland thrusting led to a viscoelastic relaxation of the Bavarian part of the Molasse foreland basin, according to Zweigel et al. (1998), which was followed by a subsidence event at the thrust front and the development of a marine connection throughout the molasse basin. The drop of sediment discharge from the Alps is interpreted in terms of a reduction of relief by Kuhlemann et al. (subm.). Alternative explanations are discussed by Schlunegger (1999).

#### 4.4. The 17 Ma event

Between 18 and 17 Ma, a short-termed, drastic increase of sediment discharge rates is observed (Fig. 9). At this time the eastern part of the Eastern Alps collided with the Bohemian spur (e.g. Decker and Peresson, 1996), which initiated the closure of the marine gateway between the central Paratethys and the Western Mediterranean (Lemcke, 1988). The Bohemian spur formed an obstacle for eastward lateral extrusion and may temporarily have prevented or at least slowed down this process (Ratschbacher et al., 1991a; Tari et al., 1992). This obstacle triggered an anticlockwise rotation of East Alpine tectonic units (Márton et al., 2000) and simultaneous pull-apart opening of the Vienna basin E of the Bohemian spur (Decker and Peresson, 1996).

Consequently, plate convergence has temporarily been transformed into predominantly vertical extrusion (Thompson et al., 1997). The rigid upper crust E of the Brenner line broke into a number of tectonic blocks which started to move towards the E along conjugate strike-slip faults which still dominate the tectonic pattern of the Eastern Alps (Frisch et al., 1998). Activity of this fault pattern and an exhumation pulse in the Tauern and Rechnitz windows around 17 Ma is well documented (Cliff et al., 1985; Blanckenburg et al., 1989; Dunkl and Demény, 1997; Läufer et al., 1997). For the Swiss Alps, an uplift event and increase of relief is also indicated by increased sediment discharge (Kuhlemann, 2000). The uplift appears to have been focussed in the region of the,

still buried, Aar massif (Schlunegger et al., 1998; Schlunegger, 1999).

#### 4.5. The middle miocene phase

Subsequent extrusion after 17 Ma is indicated by further exhumation of the Tauern core complex from middle to upper crustal levels (Genser et al., 1996). However, material of the Tauern window was not exposed before 13 Ma (Brügel, 1998; Frisch et al., 1998).

Along the extensional fault pattern a number of intramontane basins were newly formed from about 17 Ma on (see Ratschbacher et al., 1991b). In Langhian–Serravallian times the valleys east of the developing Tauern window drowned in erosional debris due to crustal thinning (Frisch et al., 1999), giving rise to a local transgression of the Paratethys. The generally low sediment discharge rates in the entire Alps between 16 and 12 Ma records further extension (Kuhlemann, 2000), which is closely linked to the extension and continental escape in the Pannonian basin (Tari et al., 1992; Tari and Horváth, 1995). Space for extensional processes was provided by accelerated roll-back of the Carpathian subduction zone between 17 and 12 Ma (Royden, 1993; Sperner, 1997).

#### 4.6. The late Miocene phase

The increase of sediment discharge rates in the Eastern Alps between 12 and 10 Ma by 35% (Kuhlemann et al., 2000) is coeval with a regional regression (Winkler-Hermaden, 1957). This change appears to be related to the onset of thrusting and uplift in the eastern Southern Alps (Schönborn, 1992; Dunkl et al., 1996; Kuhlemann, 2000), and the termination of E–W extension in the Eastern Alps (Dunkl et al., 1998). At 12 Ma, a strong increase of the size of pebbles derived from the freshly exposed Penninic material of the Tauern window indicates a sudden increase of relief in the Tauern window (Frisch et al., 1998).

### 5. Post-Eocene bulk erosion

The total amount of sediment derived from the entire Alps since Eocene times (33.7 Ma) amounts to  $\sim 876,000 \text{ km}^3$ , equivalent to a rock pile of 5.3 km thickness, calculated for the recently exposed area of the Alps.

This volume is almost identical to that calculated by Hay et al. (1992). The calculation of Guillaume and Guillaume (1984) is about 13% higher. The Eastern Alps (Southern Alps east of Lake Como excluded) account for  $\sim 216,000 \text{ km}^3$  of sediment (Kuhlemann, 2000). England (1981) has been the first to compare the thickness of missing hanging wall rock, deduced from metamorphic isograds, with Alpine derived sediment volumes. He calculated equal volumes of eroded rocks and Alpine-derived debris in the range of  $1,000,000 \text{ km}^3$ .

## 6. Erosional versus tectonic denudation

### 6.1. Tauern window

Between 22 and 12 Ma, which is the main period of lateral extrusion in the Eastern Alps,  $\sim 56,000 \text{ km}^3$  of solid rock eroded from the entire Eastern Alps were deposited in the basins. Most of this volume is derived from the area W of the Brenner line, where a relatively high relief already existed in early Miocene times (see above). Below, average erosion rates of the terrains west, east, north, and south of the Tauern window are estimated.

#### 6.1.1. West of the Tauern window

The largest catchment in the western part of the Eastern Alps belonged to the Paleo-Inn river, draining Austroalpine basement as far to the SW as the Adamello massif (Brügel, 1998). Since the Paleo-Inn catchment also included the western parts of the later Tauern window, that was covered by Austroalpine basement until 13 Ma (see above), it is not possible to differentiate between erosive products from the Austroalpine hanging wall above the western Tauern window ( $\sim 2500 \text{ km}^2$  size) and the western Austroalpine crystalline terrains. The assumption of equal erosion rates in the whole catchment of the Paleo-Inn displays a lower limit of erosion above the Tauern window, since enhanced deformation and fracturing in this area probably enhanced erosion.

The Austroalpine tectonic unit extended further to the southwest and west than today, and may have extended almost as far to the W as the recent Alpine Rhine river (Spiegel et al., 2000;  $\sim 15,000 \text{ km}^2$ ;

Fig. 10). Apatite fission track data from the western Austroalpine source terrain (Flisch, 1986; Elias, 1998) indicate that between 22 and 12 Ma an average of about 1.2 km of rock has been eroded. According to these data, a somewhat higher erosion rate is indicated by younger cooling ages for the southern and southwestern parts and lower erosion rates in the northern parts (Silvretta).

At least  $\sim 4000 \text{ km}^3$  of solid load were derived from the western Northern Calcareous Alps (presently covering  $\sim 7500 \text{ km}^2$  size; Fig. 10), since carbonate pebbles and grains of this provenance make up the bulk of the fans (Schiemenz, 1960). Suspended and dissolved load transported to farther distances are assumed to range also  $\sim 4000 \text{ km}^3$ , since the dissolved load typically represents more than 40% of the total load under recent conditions (Einsele and Hinderer, 1997).

#### 6.1.2. East of the Tauern window

For the Austroalpine basement east of the Tauern window ( $\sim 19,000 \text{ km}^2$ ) the average erosion rate is estimated around 0.04 km/My, in line with apatite fission track data of Hejl (1997). This very low erosion rate is consistent with the preservation of several Early Miocene paleorelief remnants (Frisch et al., 2000), which testify very slow surface processes in this area. The intramontane basins within this terrain were supplied from the Austroalpine hanging wall of the Tauern window, and other local sources (Exner, 1949; Polesny, 1970; Heinrich, 1977).

#### 6.1.3. North of the Tauern window

For the basement between the Tauern window and the Northern Calcareous Alps (NCA;  $\sim 3500 \text{ km}^2$ ), an average erosion of about 0.9 km is estimated between 22 and 12 Ma. In the rugged western and eastern areas the amount of erosion was rather in the range of that of the western Austroalpine basement, and probably less in the central section, as indicated by a few apatite fission track ages (Hejl, 1997).

Most of the central and eastern NCA and the flysch zone north of this unit were not subjected to erosion between 22 and 12 Ma (Frisch et al., 2000b), except for the northeasternmost part. The latter area supplied pebbly debris to the foreland basin and the Vienna basin (Tollmann, 1985). The sediment discharge from this area is estimated around  $500 \text{ km}^3$ . Sedimentation of

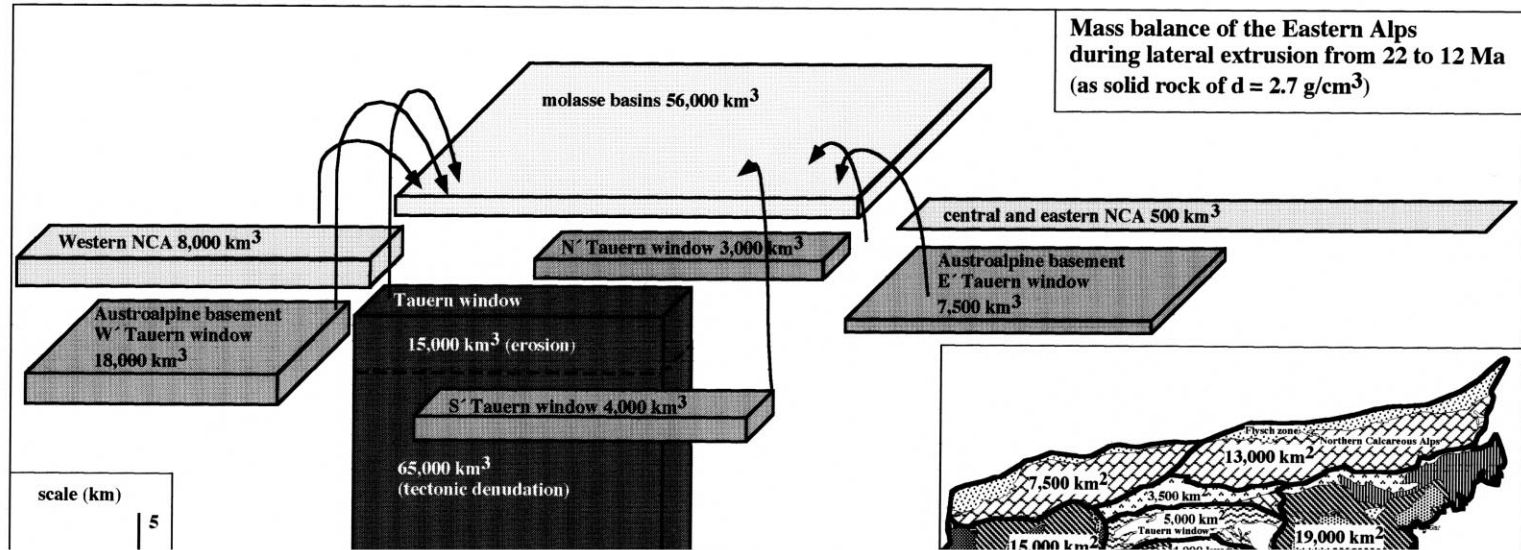


Fig. 10. Exhumation budget of the Eastern Alps and the Tauern window, and recent area size of source terrains of the Eastern Alps.

molasse debris on top of the central and eastern NCA probably lasted until 18 Ma and erosion of this siliciclastic cover after 18 Ma did not cut down to the NCA before 10 Ma (Frisch et al., 1998). The reworked volume of this molasse material until 12 Ma is in the range of  $\sim 2400 \text{ km}^3$  (Kuhlemann, 2000). The hilly relief of the central and eastern Northern Calcareous Alps covered an area of  $\sim 13,000 \text{ km}^2$ , representing  $\sim 20\%$  of the erosion area of the Eastern Alps.

#### 6.1.4. South of the Tauern window

The amount of surface erosion south of the Tauern window ( $\sim 4000 \text{ km}^2$  size) is more difficult to estimate, since Miocene apatite fission track ages (Grundmann and Morteani, 1985; Staufenberg, 1987) indicate both tectonic and erosive denudation within this Austroalpine hanging wall-unit. Low-angle normal faulting within the hanging wall-unit appears to have denuded the northern parts of this source terrain (Frisch et al., 1998). The average surface erosion is roughly estimated in the order of 1.0 km and was certainly higher in the northwestern due to rugged relief and lower particularly in the southeastern part, as indicated by few fission track data from the Schober group (Staufenberg, 1987).

If the eroded volumes of all terrains except for the area covering the later Tauern window are added ( $41,000 \text{ km}^3$ ), an eroded volume of  $\sim 15,000 \text{ km}^3$  remains to be derived from the source region of the exhuming Tauern window (Fig. 10). This is equivalent to a surface erosion rate of 0.3 mm/yr between 22 and 12 Ma.

During the extrusion period, the footwall of the Tauern window were exhumed by an average of 16 km (Blanckenburg et al., 1989). With respect to the size of  $5000 \text{ km}^2$  this means that a total volume of  $80,000 \text{ km}^3$  of solid rock has been removed from above the window. As a result, up to 20% of the exhumation of the footwall was performed by erosion, while the major part was performed by tectonic denudation. This calculation matches with the tectonic restoration (Frisch et al., 2000a).

The erosion rate of 0.3 mm/yr is twice of that calculated for the area W of the Brenner line (0.15 mm/yr). Note that more easily erodible rocks of the footwall, such as metapelites (Bünden schists) were not exposed before 13 Ma, too late to strongly modify the erosion rates during the previous 9 My.

Evidence for increased relief to explain erosion rates twice as high as compared to the tectonic frame of the Tauern window, is entirely missing. Higher erosion rates of the extensional allochthon on the evolving Tauern window can reasonably be explained by ongoing strong deformation, which potentially enhanced erodibility. However, the relative importance of either updoming and increased relief in late Early Miocene times or strong deformation cannot be determined.

#### 6.2. Lepontine dome

The estimate for the exhumation budget of the Swiss Lepontine dome is less precise than in the case of the Tauern core complex, since no differentiated sediment budgets for several parts of the Western, Swiss and western parts of the Southern Alps can be obtained (see Kuhlemann, 2000). The sediment volume derived from the whole area of  $\sim 67,000 \text{ km}^2$  by the end of the extension period sums up to  $\sim 176,000 \text{ km}^3$  between 22 and 12 Ma (Fig. 9). If average erosion rates in the entire Swiss and Western Alps between 22 and 12 Ma were similar (0.263 mm/yr), the area of  $\sim 20,000 \text{ km}^2$  of the Swiss part (between the Great St Bernhard pass and the Alpine Rhine river) would account for a sediment volume of  $\sim 53,000 \text{ km}^3$  (equivalent solid rock). This estimate displays a lower limit for the Swiss Alps, where average erosion rates are higher than in the French and Italian Western Alps, according to cooling ages (Hunziker et al., 1992). The exhumation of footwall rock from about 15 to 20 km depth, according to cooling ages between 22 and 12 Ma (Bradbury and Nolen-Hoeksema, 1985; Hunziker et al., 1992; Grasmann and Mancktelow, 1993), requires a removal of  $\sim 60,000 \text{ km}^3$  of hanging wall-rock.

The exhumation rates calculated by Schlunegger and Willett (1999) for the western, northern and eastern frame of the Lepontine dome between 22 and 12 Ma have been considered as surface erosion rates (Fig. 11). Average surface erosion rates of the Aar massif were ranging around 0.3 mm/yr, according to zircon and apatite cooling ages (Michalski and Soom, 1990). Erosion rates of the nappe pile of sediments in the Prealps are estimated around 0.2 mm/yr, due to decreasing relief towards the northern margin of the Swiss Alps. Erosion rates estimated to be 2–3 times higher in the axial part as compared to the margins of the Swiss and Western Alps roughly fit to cooling rates

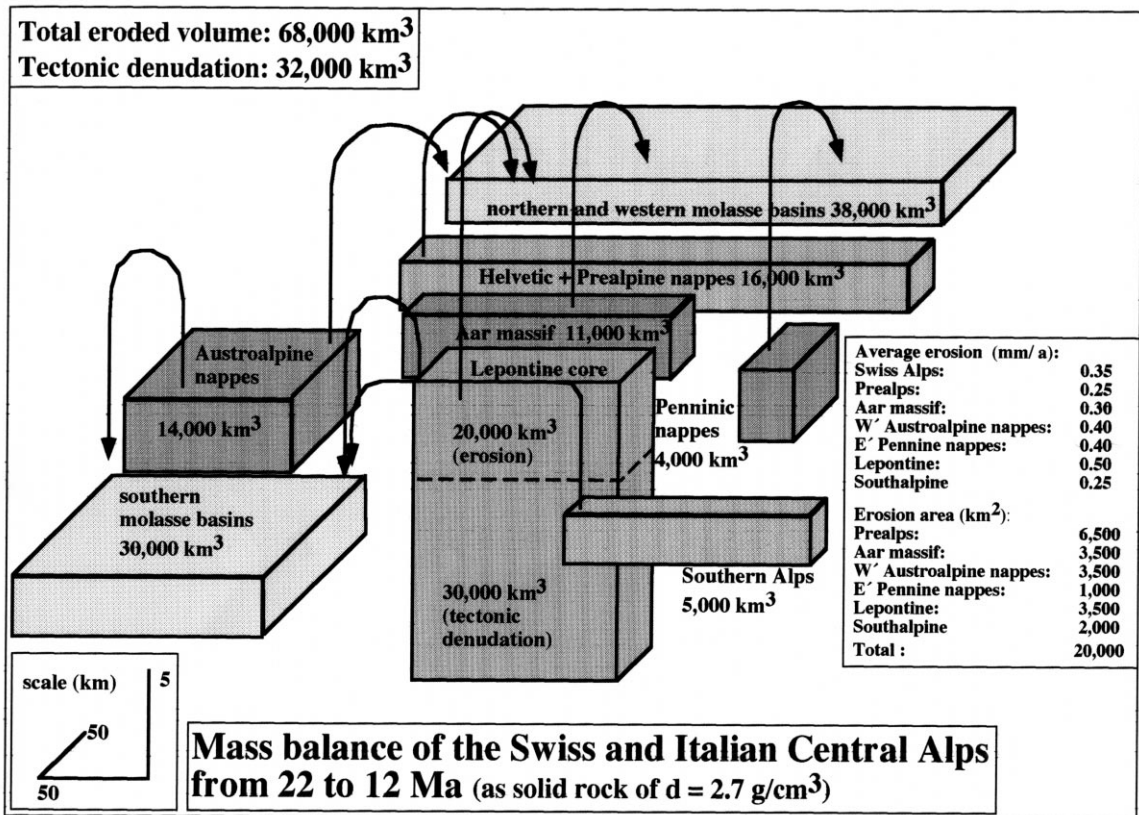


Fig. 11. Exhumation budget of the Swiss Alps and the Lepontine window, based on thermochronologic data compiled by Schlunegger and Willett (1999).

and the metamorphic pattern, compiled by Hunziker et al. (1992). The Penninic nappes W and E of the Lepontine dome were partly covered by Austroalpine basement (Pfiffner, 1986), where cooling paths indicate erosion rates of  $\sim 0.4 \text{ mm/yr}$ . These erosion rates would produce  $\sim 50,000 \text{ km}^3$  of sediment between 22 and 12 Ma, derived from the structural frame of the Lepontine dome.

Cooling paths of the Lepontine dome and age distribution maps compiled by Schlunegger and Willett (1999) indicate that rapid exhumation of particular segments within the dome concentrated in a period of 5 My (Fig. 12), and that the zone of rapid exhumation migrated from the E to the W. On the base of cooling paths, modelled by Schlunegger and Willett (1999), it is assumed that the denudation of the Lepontine dome prior to tectonic unroofing ( $\sim 30\text{--}22 \text{ Ma}$ ;  $\sim 0.6 \text{ mm/yr}$ ) and after the main phase of tectonic unroofing

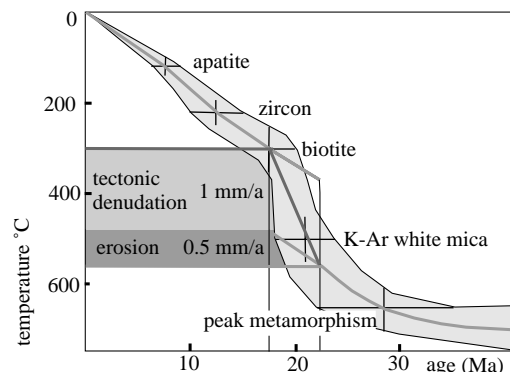


Fig. 12. Exhumation path of the Lepontine core, redrawn after Schlunegger and Willett (1999), and graphic construction of the contribution of tectonic denudation.

(12–5 Ma;  $\sim 0.4$  mm/yr), was due to surface erosion. This average matches the average trend of sediment discharge of the Swiss and Western Alps (see Fig. 9) between 30 and 5 Ma, but certainly the sediment budget method cannot resolve regionally deviating trends. If an average surface erosion rate of  $\sim 0.5$  mm/yr is accepted, its multiplication with the time of 10 My and the area size of the Lepontine dome results in a volume of  $\sim 18,000$  km<sup>3</sup>.

Adding the sediment volume of  $\sim 18,000$  km<sup>3</sup>, derived from the hanging wall of the Lepontine dome, to the sediment volume derived from the frame of the Lepontine dome ( $\sim 47,000$  km<sup>3</sup>), a bulk sediment volume of  $\sim 65,000$  km<sup>3</sup> derived from the Swiss Alps between 22 and 12 Ma. This volume estimate exceeds the minimum volume, calculated to be  $\sim 53,000$  km<sup>3</sup> for the average of the entire Swiss and Western Alps (see above) by  $\sim 12,000$  km<sup>3</sup>. Average erosion rates of 0.33 mm/yr in the Swiss Alps as compared to 0.24 mm/yr in the Western Alps between 22 and 12 Ma are in line with the general cooling pattern (see Hunziker et al., 1992).

The sediment budget of the Swiss and western Alps, however, is not precise enough and has poor regional resolution as to independently support or contradict estimates of tectonic denudation in the case of the Lepontine dome. This is due to the fact that, in contrast to the Eastern Alps, the bulk sediment volume derived from the Swiss and Western Alps by far exceeds the volume of hanging wall removed from the Lepontine dome. In this case an estimate of tectonic versus erosive denudation is based on the exhumation path alone (Fig. 12).

The amount of exhumation in excess of 0.5 mm/yr of erosion between 22 and 12 Ma, which is  $\sim 1$  mm/yr in average, is interpreted to be due to tectonic denudation (Fig. 12). Thus, the exhumation of the Lepontine core complex from 22 to 12 Ma is probably dominantly ( $\sim 70\%$ ) the result of tectonic denudation, equivalent to a volume of  $\sim 42,000$  km<sup>3</sup> of tectonically removed hanging wall rock. This is only  $\sim 24\%$  of the volume eroded in the Swiss and Western Alps and thus still within the error range of the sediment budget method. This might be the reason why models of cooling and erosion cannot unequivocally resolve the problem to differentiate between exhumation by surface erosion alone, or by a combination of tectonic denudation and surface erosion (Schlunegger and Willett, 1999).

### 6.3. Rechnitz window

In the Rechnitz window, Penninic footwall was exhumed from about 10 km depth between 22 and 12 Ma (Koller, 1985; Dunkl and Demény, 1991; Dunkl and Demény, 1997). Some 5000 km<sup>3</sup> of hanging wall has been removed from an area of  $\sim 500$  km<sup>2</sup>. Synrift sediments of the hanging wall, covering the Penninic footwall, still reach a thickness of 1 km in places and are thermally overprinted by the heat of the exhuming footwall (Dunkl et al., 1998). As a result of crustal thinning between 22 and 12 Ma, the core complex formed during overall subsidence and was buried under more than 2 km thick sediments, mostly removed today (Dunkl et al., 1998). Thus, exhumation was almost exclusively performed by tectonic denudation.

## 7. Conclusion

Tectonic denudation in the Alps accounts for  $\sim 65,000$  km<sup>3</sup> of exhumation in the Tauern window,  $\sim 42,000$  km<sup>3</sup> in the Lepontine window, and  $\sim 5000$  km<sup>3</sup> in the Rechnitz window. Exhumation by extension in the Engadine window, and other small areas of minor importance (e.g. Pohorje; Fodor et al., 1998) may together account for about 5000–10,000 km<sup>3</sup> of denudation. Between 22 and 12 Ma  $\sim 34\%$  of the overall exhumation of the entire Alps has been performed by tectonic denudation ( $\sim 120,000$  km<sup>3</sup>).

Since tectonic denudation occurred also before 22 Ma, e.g. in the Italian Western Alps (Sesia-Lanzo zone and the Dora Maira massif), a maximum of  $\sim 88\%$  of exhumation of the entire Alps since Oligocene times has been performed by surface erosion, whereas tectonic denudation accounts for a minimum of  $\sim 12\%$  of the overall exhumation.

In the case of the Tauern window,  $\sim 80\%$  of the exhumation of the footwall is accounted to tectonic denudation.

In the Alps, the period of lateral extrusion and tectonic denudation is generally a period of reduced erosion, due to reduced relief. Nevertheless, the extensional phase between 22 and 12 Ma was interrupted by a short period of updoming and increased relief in late Early Miocene times. Erosion rates of the hanging wall cover of the evolving core

complex, however, appear to be higher than elsewhere in the Eastern Alps.

The sediment budget of an orogen potentially provides an independent data base for quantitative estimates of exhumation processes, complementary to thermochronologic data. The sediment budget method can be successfully applied, if the rock volume to be removed from above an exhuming core complex exceeds the volume of contemporaneously deposited debris.

**Acknowledgements**

This study has been funded by Collaborative Research Center (SFB) 275 financed by the Deutsche

Forschungsgemeinschaft. M. Kázmér and A. Di Giulio provided sediment budget data and hardly accessible literature from the Pannonian basin and the Apeninnes, respectively. The paper benefited much from constructive reviews of L. Ratschbacher and F. Schlunegger and additional comments of J.-P. Burg. All support is gratefully acknowledged.

**Appendix A**

The compilation of sediment discharge from the Eastern Alps to all adjacent basins is shown in Table A1.

The chart of the data flow of the processing is shown in Fig. A1.

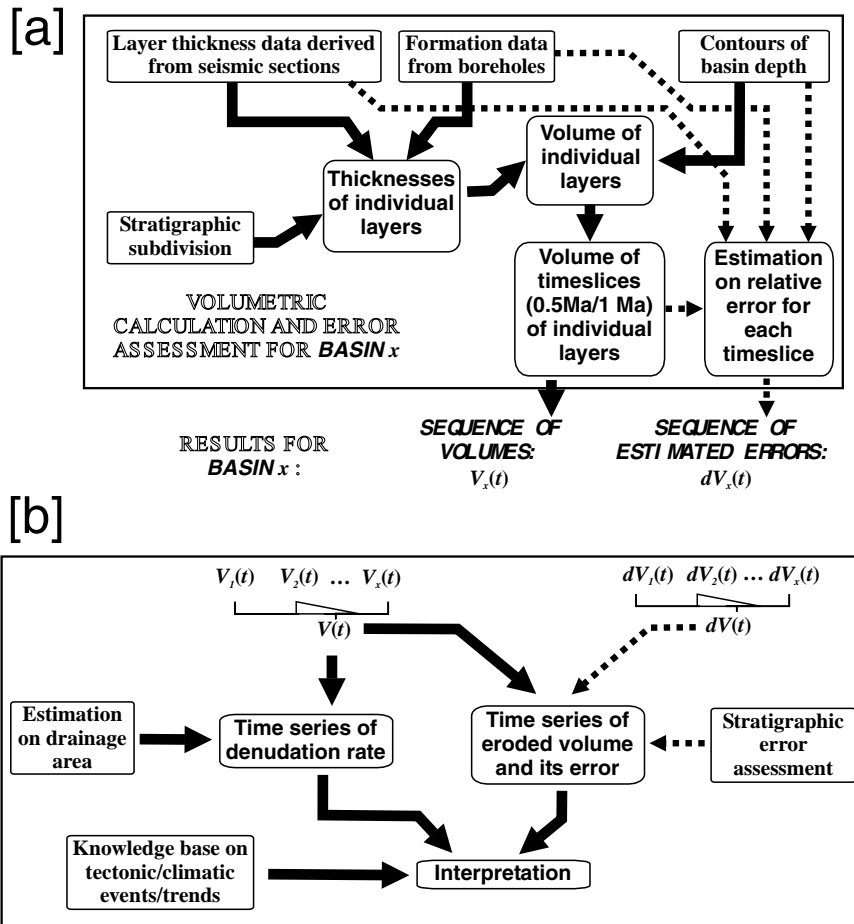


Fig. A1. Chart of the data flow of the processing. Solid arrows indicate data flow, dotted ones represent error propagation calculations. Data within rounded boxes are derivatives of raw data (within frames) and other derivatives.

Table A1

Compilation of sediment discharge from the Eastern Alps to all adjacent basins. The key for the relative error is related to the single volume in km<sup>3</sup> of solid rock. Note that the error of 100% indicates that we cannot be sure if during a given period of 0.5 My (e.g. 24.5–24.0 Ma) sediment has definitely been deposited. If it was not, at some other time more sediment was deposited. The error of the formation as a whole (e.g. Augenstein formation) is much less, but still ~50%

Sediment mass (km <sup>3</sup> )																		
Time (Ma)	GER	TVF	IBR	AUG	LAU	VIE	PAN	STY	LAV	NOR	KLA	SLO	MOE	BLA	RHO	RHI	PO	CH
0.5							1300						5	300	6000	1400	1200	
1.0							1150						5	300	5200	1200	1100	
1.5							1000						5	300	4200	300	700	1000
2.0							1050						5	600	2700	800		800
2.5							1750						5	1000	1300	800		650
3.0							2250					5	5	1200	500	800		550
3.5							2850					5	5	1200		400		500
4.0							3250					5	5	800				500
4.5							3650					5						450
5.0							3850	5				10		100				350
5.5							3900	10				10						300
6.0	90					10	3850	10				30						300
6.5	200					10	3750	10				30						300
7.0	300					20	3700	10				35						300
7.5	450					30	3550	20				35						250
8.0	500					40	3450	20				40						250
8.5	550					50	3300	20				40						250
9.0	650					60	3250	20	5			40						200
9.5	650					70	3050	20	5			40						200
10.0	700					80	2850	20	5			40	20					200
10.5	750					130	1750	25	5			40	30		500			200
11.0	650					140	1450	25	5			40	30		800			150
11.5	300					150	850	30	5			40	30		1500			100
12.0	190				10	230	150	250	10			50	30		1700			70
12.5	190				10	230	150	250	10			50	30		1750			80
13.0	190				20	230	150	250	15			30	30		1750			100
13.5	600				20	220	150	100	17	10		30			1500			100
14.0	700				20	220	150	100	17	20		30			1400			100
14.5	700				20	220	150	110	17	40		30			1400			100
15.0	750				20	220	150	110	17	50		30			1350			100
15.5	800				20	230	150	110	17	60		30			1300			100
16.0	850				30	280	160	120	17	70		30			1250			100
16.5	1040				250	400	220	150	18	90		30			1050			100
17.0	1300			100	1100	900	230	700	30	110		30			800			
17.5	1300			100	1100	750	240	450	10	270		30			300			
18.0	1300			40	1100	150	250	300		80		30			300			
18.5	600	100		0	250	50	500								250			
19.0	500	100		50	240	30	550								200			
19.5	400	150	5	200	230	20	550								200			
20.0	300	200	5	300	220		550								200			
20.5	250	250	20	300	200		410								200			
21.0	1250	200	20	400	150		300											
21.5	2400		30	350	150		280											
22.0	2300		20	300	100		280											
22.5	2200		20	300	100		280											
23.0	2100		20	300	90		270											
23.5	2000		20	300	80		270											
24.0	1900		20	300	70		270											
24.5	1800		20	350	50		270											
25.0	1800		20	350	50		270											
25.5	1800		20	300	50		270											
26.0	1800		20	300	50		280											
26.5	1800		20	300	50		280											
27.0	1800		20	150	50		300											
27.5	1800		20	50	50		350											
28.0	1600		20		50		350											
28.5	1100		20		50		450											
29.0	800		15		50		450											
29.5	800		15		50		450											
30.0	800		15		50		450											
30.5	800		15		50		320											
31.0	800		15		50		200											
31.5	800		15		30		90											
32.0	800		10		20		70											
32.5	850		10		20		70											
33.0	850		10		20		70											
33.5	850		10		10		70											
34.0	850		10		0		70											
km <sup>3</sup>	56200	1000	500	5140	6400	5170	72740	3245	230	800	620	540	5800	19902	22800	3300	10200	1000

Key: **bold** 20%  
**bold** 30%  
*italic* 40%  
normal 50%  
strike 100%

Key for Alpine-adjacent basins, as partly displayed by Fig. 4: GER = German (and Upper Austrian) molasse basin; TVF = temporary valley fill; IBR = Inntal basin relics; AUG = Augenstein-Fm.; LAU = Lower Austrian molasse basin; VIE = Vienna basin; PAN = Pannonian basin; STY = Styrian basin; NOR: Noric depression; KLA = Klagenfurt basin; SLO = Slovenian basin s.l.; MOE = Moesia or Moesian platform; BLA = Black Sea/Danube fan; RHO = Rhône fan; RHI = Rhine delta, Channel and North Sea; PO = Po plain/Adriatic Sea; CH = Swiss molasse basin).

## References

- Berggren, W.A., Kent, D., Swisher, C.C., III, Aubry, M.-P., 1995. A revised Cenozoic geochronology and chronostratigraphy. *SEPM Spec. Publ.* 54, 129–212.
- Bevington, P.R., 1969. *Data Reduction and Error Analysis for the Physical Sciences*. McGraw-Hill, New York.
- Blanckenburg, F.V., Villa, I.M., Baur, H., Morteani, G., Steiger, R.H., 1989. Time calibration of a PT-path from the Western Tauern Window, Eastern Alps: the problem of closure temperatures. *Contrib. Mineral. Petrol.* 101, 1–11.
- Blanckenburg, F.V., Davies, J.H., 1995. Slab breakoff: a model for syncollisional magmatism and tectonics in the Alps. *Tectonics* 14, 120–131.
- Bradbury, H.J., Nolen-Hoeksema, R.G., 1985. The Lepontine Alps as an evolving metamorphic core complex during A-type subduction: evidence from heat flow, mineral cooling ages, and tectonic modelling. *Tectonics* 4, 187–211.
- Brandon, M.T., Vance, J.A., 1992. Tectonic evolution of the Cenozoic Olympic subduction complex, Washington State, as deduced from fission track ages for detrital zircons. *Am. J. Sci.* 292, 565–636.
- Brügel, A., 1998. Provenance of alluvial conglomerates from the Eastalpine foreland: oligo-/Miocene denudation history and drainage evolution of the Eastern Alps. *Tübinger Geowiss. Arb.*, Ser. A 40, 168 pp.
- Brügel, A., Dunkl, I., Frisch, W., Kuhlemann, J., Balogh, K., 2000. Geochemistry and geochronology of the gneiss pebbles of the eastern Alpine Molasse: geodynamic and paleogeographic implications for the Oligomiocene evolution. Submitted Mem. *Sci. Geol.* (Padova).
- Brunel, M., Arnaud, N., Tapponnier, P., Pan, Y., Wang, Y., 1994. Kongur Shan normal fault; type example of mountain building assisted by extension Karakoram Fault, eastern Pamir. *Geology* 22 (8), 707–710.
- Burg, J.-P., Davy, P., Nievergelt, P., Oberli, F., Seward, D., Diao, Z., Meier, M., 1997. Exhumation during crustal folding in the Namche–Barwa syntaxis. *Terra Nova* 9, 53–56.
- Cliff, R.A., Droop, G.T.R., Rex, D.C., 1985. Alpine metamorphism in south-east Tauern Window, Austria: 2. Rates of heating, cooling and uplift. *J. Metamorphic Geol.* 3, 403–415.
- Daly, R.A., Manger, G.E., Clark Jr., S.P., 1966. Density of rocks, sec. 4. In: *Handbook of Physical Constants*, revised edition. *GSA Mem.*, pp. 19–26.
- Decker, K., Peresson, H., 1996. Tertiary kinematics in the Alpine–Carpathian–Pannonian System; links between thrusting, transform faulting and crustal extension. Wessely, G., Liebl, W. (Eds.), *Oil and gas in Alpidic thrust belts and basins of Central and Eastern Europe*. *EAPG Spec. Publ.* 5, 69–77.
- Dunkl, I., Demény, A., 1997. Exhumation of the Rechnitz Window at the border of the Eastern Alps and the Pannonian basin during Neogene extension. *Tectonophysics* 272, 197–211.
- Dunkl, I., Picotti, V., Selli, L., Castellarin, A., Frisch, W., 1996. Low temperature thermal history of the Dolomites. Preliminary results. Abstract 78th Congress of the Geological Society of Italy in St Cassiano, Rome, 16–18, September.
- Dunkl, I., Grasemann, B., Frisch, W., 1998. Thermal effect on upper plate during core-complex denudation: a case study from the Rechnitz Window, Eastern Alps. *Tectonophysics* 297, 31–50.
- Dunkl, I., Frisch, W., Grundmann, G., 2000a. Zircon fission track thermochronology of the southeastern part of the Tauern Window and the adjacent Austroalpine margin. Submitted *Ecol. Geol. Helv.*
- Dunkl, I., Frisch, W., Kuhlemann, J., Brügel, A., 2000b. Pebble population dating (PPD) — a new method for provenance research using single grain fission track chronology on amalgamated pebble populations. Submitted for publication.
- Einsele, G., Hinderer, M., 1997. Terrestrial sediment yield and life-times of reservoirs, lakes, and larger basins. *Geol. Rundschau*, 86, 288–310.
- Einsele, G., Ratschbacher, L., Wetzel, A., 1996. The Himalaya–Bengal fan denudation–accumulation system during the past 20 Ma. *J. Geol.* 104, 163–184.
- Elias, J., 1998. The thermal history of the Ötztal–Stubai complex (Tyrol, Austria/Italy) in the light of the lateral extrusion model. *Tübinger Geowiss. Arb.*, Ser. A 36, 172 pp.
- England, P.C., 1981. Metamorphic pressure estimates and sediment volumes for the Alpine orogeny: an independent control on geobarometers?. *Earth Planet. Sci. Lett.* 56, 387–397.
- England, P.C., Molnar, P., 1990. Surface uplift, uplift of rocks, and exhumation of rocks. *Geology* 18, 1173–1177.
- Exner, C., 1949. Beitrag zur Kenntnis der jungen Hebung der östlichen Hohen Tauern. *Mitt. Geogr. Ges. Wien.* 91, 186–196.
- Fodor, L., Jelen, B., Márton, E., Skaberne, D., Car, J., Vrabec, M., 1998. Miocene–Pliocene tectonic evolution of the Slovenian Periadriatic fault — implications for Alpine–Carpathian extrusion models. *Tectonics* 17, 690–709.
- Flisch, M., 1986. Die Hebungsgeschichte der oberostalpinen Silvretta-Decke seit der mittleren Kreide. *Bull. Ver. Schweiz. Petrol.-Geol. Ing.* 53 (123), 23–49.
- Foster, D.A., John, B.E., 1999. Quantifying tectonic exhumation in an extensional orogen with thermochronology: examples from the southern Basin and Range Province. Ring, U., Brandon, M.T., Lister, G.S., Willett, S.D. (Eds.), *Exhumation Processes: Normal Faulting, Ductile Flow and Erosion*. *Geol. Soc. London Spec. Publ.* 154, 343–364.
- Frank, W., Kralik, M., Scharbert, S., Thoeni, M., 1987. Geochronological data from the eastern Alps. In: Fluegel, H.W., Faupl, P. (Eds.), *Geodynamics of the Eastern Alps*. *Franz Deuticke, Vienna*, pp. 272–281.
- Frisch, W., Kuhlemann, J., Dunkl, I., Brügel, A., 1998. Palinspastic reconstruction and topographic evolution of the Eastern Alps during late Tertiary tectonic extrusion. *Tectonophysics* 297, 1–15.
- Frisch, W., Brügel, A.J., Dunkl, I., Kuhlemann, J., Satir, M., 1999. Post-collisional large-scale extension and mountain uplift in the Eastern Alps. *Mem. Sci. Geol. Padova* 51, 3–23.
- Frisch, W., Székely, B., Kuhlemann, J., Dunkl, I., 2000. Geomorphological evolution of the Eastern Alps in response to Miocene tectonics. *Z. Geomorph. NF* 44, 103–138.
- Frisch, W., Dunkl, I., Kuhlemann, J., 2000a. Postcollisional orogen-parallel large-scale extension in the Eastern Alps. *Tectonophysics*, 327, 239–265.
- Frisch, W., Kuhlemann, J., Dunkl, I., Székely, B., Juhász, A., 2000b.

- The Dachstein paleosurface and the Augenstein formation in the Northern Calcareous Alps — a mosaicstone in the geomorphological evolution of the Eastern Alps. *Int. J. Earth Sci.*, in press.
- Fügenschuh, B., Seward, D., Mancktelow, N., 1997. Exhumation in a convergent orogen: the western Tauern window. *Terra Nova* 9, 213–217.
- Genser, J., Van Wees, J.D., Cloething, S., Neubauer, F., 1996. Eastern Alpine tectono-metamorphic evolution: constraints from two-dimensional P–T–t modeling. *Tectonics* 15, 584–604.
- Grasemann, B., Mancktelow, N.S., 1993. Two dimensional thermal modelling of normal faulting: the Simplon fault zone, Central Alps, Switzerland. *Tectonophysics* 225, 155–165.
- Grundmann, G., Morteani, G., 1985. The young uplift and thermal history of the central Eastern Alps (Austria/Italy), evidence from apatite fission track ages. *Geol. Jahrb. B.-A.* 128, 197–216.
- Guillaume, A., Guillaume, S., 1984. L'érosion dans les Alpes au Plio-Quaternaire et au Miocène. *Eclogae. Geol. Helv.* 75, 247–268.
- Harland, W.B., Armstrong, R.L., Cox, A.V., Craig, L.E., Smith, A.G., Smith, D.G., 1989. *A Geologic Time Scale*. Cambridge University Press, UK, 263 pp.
- Heinrich, M., 1977. Zur Geologie des Tertiärbeckens von Tamsweg mit kristalliner Umrahmung. *Jahrb. Geol. B.-A.*, Wien 120, 295–341.
- Hejl, E., 1997. “Cold spots” during the Cenozoic evolution of the Eastern Alps; thermochronological interpretation of apatite fission-track data. *Tectonophysics* 272, 159–173.
- Hay, W.H., Wold, C.N., Herzog, J.M., 1992. Preliminary mass-balanced, 3D reconstructions of the Alps and surrounding areas during the Miocene. In: Pflug, R., Harbough, J.W. (Eds.), *Computer graphics in Geology*. Lecture notes in Earth Sciences, vol. 41., pp. 99–110.
- Homewood, P., Allen, P.A., Williams, G.D., 1986. Dynamics of the Molasse basin of western Switzerland. *Spec. Publ. Int. Assoc. Sediment.* 8, 199–217.
- Hunziker, J.C., Desmons, J., Hurford, A.J., 1992. Thirty-two years of geochronological work in the Central and Western Alps: a review on seven maps. *Mém. Géol.* 13, 59 pp. (Lausanne).
- Hunziker, J.C., Hurford, A.J., Calmbach, L., 1997. Alpine cooling and uplift. In: Pfiffner, O.A., Lehner, P., Heitzmann, P., Mueller, S., Steck, A. (Eds.), *Deep Structure of the Alps, Results of NRP 20*. Birkhäuser, Basel, pp. 260–264.
- Kempf, O., Matter, A., 1999. Magnetostratigraphy and depositional history of the upper freshwater Molasse (OSM) of eastern Switzerland. *Eclogae. Geol. Helv.* 92, 97–103.
- Kempf, O., Bolliger, T., Kälän, D., Engeser, B., Matter, A., 1997. New magnetostratigraphic calibration of Early to Middle Miocene mammal biozones of the north Alpine foreland basin. In: Aguilar, J.-P., Legendre, S., Mischeaux, J., (Eds.), *Actes du Congrès Biochrom'97*. *Mém. Trav. E.P.H.E., Inst. Montpellier*, vol. 21, pp. 547–561.
- Kempf, O., Matter, A., Burbank, D.W., Mange, M., 1999. Depositional and structural evolution of a foreland basin margin in a magnetostratigraphic framework: the eastern Swiss Molasse basin. *Int. J. Earth Sci.* 88, 253–275.
- Koller, F., 1985. Petrologie und Geochemie der Ophiolite des Penninikums am Alpenostrand. *Jahrb. Geol. B.-A.*, Wien 128, 83–150.
- Kuhlemann, J., 2000. Post-collisional sediment budget of circum-Alpine basins (Central Europe). *Mem. Sci. Geol. Padova* subm.
- Kuhlemann, J., Frisch, W., Székely, B., Dunkl, I., Kázmér, M., 2000. Post-collisional sediment budget history of the Alps: tectonic versus climatic control. *Eclog. Geol. Helv.*
- Lemcke, K., 1988. *Das bayerische Alpenvorland vor der Eiszeit. Geologie von Bayern I*. Schweizerbart, Stuttgart (175pp.).
- Läufer, A., Frisch, W., Steinitz, G., Loeschke, J., 1997. Exhumed fault-bounded Alpine blocks along the Periadriatic lineament: the Eder unit (Carnic Alps, Austria). *Geol. Rundschau* 86, 612–626.
- Lister, G.S., Banga, G., Feenstra, A., 1984. Metamorphic core complexes of Cordilleran type in the Cyclades, Aegean Sea, Greece. *Geology* 12/4, 221–225.
- Mancktelow, N., 1985. The Simplon line; a major displacement zone in the western Lepontine Alps. *Eclogae. Geol. Helv.* 78, 73–96.
- Mancktelow, N., Grasemann, B., 1997. Time-dependent effects of heat advection and topography on cooling histories during erosion. *Tectonophysics* 270, 167–195.
- Mangelsdorf, J., 1977. Der Deltaschuttkegel der Tiroler Ache. In: O., Ganss, *Geologische Karte von Bayern 1:25000*. Erläuterungen zum Blatt Nr. 8140 Prien a. Chiemsee und zum Blatt Nr. 8141 Traunstein. pp. 269–273, Verl. Bayr. Geol. Landesamt, München.
- Márton, E., Kuhlemann, J., Frisch, W., Dunkl, I., 2000. Miocene rotations in the Eastern Alps—paleomagnetic results from intramontane basin sediments. *Tectonophysics* 323, 163–182.
- Michalski, I., Soom, M., 1990. The Alpine thermo-tectonic evolution of the Aar and Gotthard massifs, Central Switzerland: fission track ages on zircon and apatite and K–Ar mica ages. *Schweizer. Mineral. Petrogr. Mitt.* 70, 373–387.
- Milliman, J.D., Syvitski, J.P.M., 1992. Geomorphic/tectonic Control of Sediment discharge to the Ocean: the importance of small mountainous rivers. *J. Geol.* 100, 525–544.
- Odin, G.S., 1994. Geological time scale (1994). *C. R. Acad. Sci. Paris II* 318, 59–71.
- Odin, G.S., Montanari, A., Coccioni, R., 1997. Chronostratigraphy of Miocene stages: a proposal for the definition of precise boundaries. *Bull. Liais. Inform. IUGS Subcom. Geochronol.* 14, 52 pp.
- Oxburgh, E.R., Lambert, R., Baadsgaard, H., Simons, J.G., 1966. Potassium–argon age studies across the southeast margin of the Tauern window, the Eastern Alps. *Verh. Geol. B.-A.*, Wien, 17–33.
- Pfiffner, O.A., 1986. Evolution of the north Alpine foreland basin in the central Alps. *Int. Assoc. Sedimentol. Spec. Publ.* 8, 219–228.
- Pittman, E.D., Larese, R.E., 1991. Compaction of lithic sands: experimental results and applications. *Am. Assoc. Petrol. Geol., Bull.* 75, 1279–1299.
- Polesny, H., 1970. Beitrag zur Geologie des Fohnsdorf-Knittelfelder und Seckauer Beckens. Unpublished PhD thesis, University of Vienna, 233 pp.
- Ratschbacher, L., Behrmann, J.H., Pahr, A., 1990. Penninic windows at the eastern end of the Alps and their relation to the intra-Carpathian basins. *Tectonophysics* 172, 91–105.

- Ratschbacher, L., Merle, O., Davy, P., Cobbold, P., 1991a. Lateral extrusion in the Eastern Alps, part 1: boundary conditions and experiments scaled for gravity. *Tectonics* 10, 245–256.
- Ratschbacher, L., Frisch, W., Linzer, H.G., Merle, O., 1991b. Lateral extrusion in the Eastern Alps; part 2, structural analysis. *Tectonics* 10, 257–271.
- Reddy, S.M., Cliff, R.A., East, R., 1993. Thermal history of the Sonnblick Dome, south-east Tauern Window, Austria: implications for heterogeneous uplift within the Pennine basement. *Geol. Rundschau* 82, 667–675.
- Reinecker, J., 2000. Stress and deformation: Miocene to present-day tectonics in the Eastern Alps. *Tübinger Geowiss. Arb., Ser. A*, 55 128 pp.
- Rögl, F., 1996. Stratigraphic correlation of the paratethys Oligocene and Miocene. *Mitt. Ges. Geol. Bergbaustud. Österr.* 41, 65–73.
- Royden, L.H., 1993. Evolution of retreating subduction boundaries formed during continental collision. *Tectonics* 12, 629–638.
- Ryan, W.B.F., Cita, M.B., 1978. The nature and distribution of Messinian erosional surfaces — indications of a several-kilometer-deep Mediterranean in the Miocene. *Mar. Geol.* 27, 193–230.
- Schiemenz, S., 1960. Fazies und paläogeographie der subalpinen Molasse zwischen Bodensee und Isar. *Beih. Geol. Jb.* 38, 1 119 pp (Hannover).
- Schlunegger, F., 1999. Controls of surface erosion on the evolution of the Alps: constraints from the stratigraphies of the adjacent foreland basins. *Int. J. Earth Sci.* 88, 285–304.
- Schlunegger, F., Willett, S., 1999. Spatial and temporal variations of exhumation of the Central Swiss Alps and implications for exhumation mechanisms. *Geol. Soc. London Spec. Publ.* 54, 157–180.
- Schlunegger, F., Burbank, D.W., Matter, A., Engesser, A., Mödden, C., 1996. Magnetostratigraphic calibration of the Oligocene to Middle Miocene (30–15 Ma) mammal biozones and depositional sequences of the Swiss molasse basin. *Eclogae Geol. Helv.* 89, 753–788.
- Schlunegger, F., Matter, A., Burbank, D.W., Klaper, E.M., 1997. Magnetostratigraphic constraints on relationships between evolution of the central Swiss Molasse basin and Alpine orogenic events. *Geol. Soc. Am. Bull.* 109, 225–241.
- Schlunegger, F., Jordan, T.E., Klaper, E., 1998. Controls of erosional denudation in the orogen on foreland basin evolution: the Oligocene central Swiss Molasse Basin as an example. *Tectonics* 16, 823–840.
- Schmid, S.M., Froitzheim, N., 1993. Oblique slip and block rotation along the Engadine line. *Eclogae Geol. Helv.* 86, 569–593.
- Schmid, S.M., Pfiffner, O.A., Schönborn, G., Froitzheim, N., Kissling, E., 1997. Integrated cross section and tectonic evolution of the Alps along the eastern traverse. In: Pfiffner, O.A., Lehner, P., Heitzmann, P., Mueller, S., Steck, A. (Eds.). *Deep Structure of the Alps, Results of NRP 20*. Birkhäuser, Basel, pp. 289–304.
- Schönborn, G., 1992. Alpine tectonics and kinematic models of the central Southern Alps. *Mem. Sci. Geol. Padova* 44, 229–393.
- Schröder, K.W., Theune, C., 1984. Feststoffabtrag und Staurationverlandung in Mitteleuropa. *Wasserwirtschaft* 74, 374–379.
- Silverstone, J., 1988. Evidence for east–west crustal extension in the Eastern Alps. *Tectonics* 7, 87–105.
- Sinclair, H.D., 1997. Flysch to molasse transition in peripheral foreland basins: The role of the passive margin versus slab breakoff. *Geology* 25, 1123–1126.
- Skeries, W., Troll, G., 1991. Der Geröllbestand in den Molassekonglomeraten des Chiemgaus (Bayern) und seine paläogeographischen Beziehungen zum alpinen Liefergebiet. *Z. Dt. Geol. Ges.* 142, 43–66.
- Sommer, N., 1980. Untersuchungen über die Geschiebe- und Schwebstoffführung und den Transport von gelösten Stoffen in Gebirgsbächen der Ostalpen. *Interprevent-Meeting, Bad Ischl.*, vol. 2, pp. 69–95.
- Sperner, B., 1997. Computer programs for the kinematic analysis of brittle deformation structures and the tertiary tectonic evolution of the Western Carpathians (Slovakia). *Tübinger Geowiss. Arb., Ser. A* 27, 120 pp.
- Spiegel, C., Kuhlemann, J., Dunkl, I., Frisch, W., von Eynatten, H., Kadosa, B., 2000. Erosion history of the Swiss Central Alps — evidence from zircon fission track data on the foreland basin sediments. *Terra Nova*, in press.
- Sprefaco, M., Lehmann, C., 1994. Sediment transport observations in Switzerland. In: *Proceedings of the Canberra Symposium, December 1994: Variability in Stream Erosion and Sediment Transport*, IAHS Publ., vol. 224, pp. 259–268.
- Staufenberg, H., 1987. Apatite fission-track evidence for postmetamorphic uplift and cooling history of the eastern Tauern window and the surrounding Austroalpine (central Eastern Alps, Austria). *Jahrb. Geol. B.-A., Wien* 130, 571–586.
- Steck, A., Hunziker, J., 1994. The tertiary structural and thermal evolution of the Central Alps — compressional and extensional structures in an orogenic belt. *Tectonophysics* 238, 229–254.
- Steininger, F.F., Bernor, R.L., Fahlbusch, V., 1990. European Neogene marine–continental chronologic correlations. In: Linsay, E.H., Fahlbusch, V., Mein, P. (Eds.), *European Neogene Mammal Chronology*. NATO ASI Ser. A, vol. 180. Plenum, New York, pp. 15–46.
- Steininger, F.F., Berggren, W.A., Kent, D.V., Bernor, R.L., Sen, S., Agustí, J., 1996. Circum-Mediterranean Neogene (Miocene and Pliocene) marine–continental chronologic correlations of European mammal units and zones. In: Bernor, R.L., Fahlbusch, V., Rietschel, S. (Eds.), *Late Neogene Biotic Evolution and Stratigraphic Correlation*. Columbia University Press, New York, pp. 64–77.
- Tari, G., Horváth, F., 1995. Middle Miocene extensional collapse in the Alpine–Pannonian transition zone. In: Horváth, F., Tari, G., Bokor, C. (Eds.), *Extensional Collapse of the Alpine Orogen and Hydrocarbon Prospects in the Basement and Basin Fill of the Western Pannonian Basin*. *Am. Assoc. Petrol. Geol. International Conference, Nice, Guidebook to field-trip No. 6*, 75–105.
- Tari, G., Horváth, F., Rumpler, J., 1992. Styles of extension in the Pannonian basin. *Tectonophysics* 208, 203–219.
- Tari, G., Dövényi, P., Dunkl, I., Horváth, F., Lenkey, L., Stefanescu, M., Szafián, P., Tóth, T., 1999. Lithospheric structure of the Pannonian basin derived from seismic, gravity and geothermal data. In: Durand, B., Jolivet, L., Horváth, F., Séranne, M. (Eds.),

- The Mediterranean basins: Tertiary extension within the Alpine orogen. *Geol. Soc. London Spec. Publ.* 156, 215–250.
- Thompson, A.B., Schulmann, K., Jezek, J., 1997. Extrusion tectonics and elevation of lower crustal metamorphic rocks in convergent orogens. *Geology* 25, 491–494.
- Tollmann, A., 1985. *Geologie von Österreich. Band II. Außerzentralalpiner Anteil.* Deuticke, Vienna, 710 pp.
- Tucker, G.E., Slingerland, R., 1996. Predicting sediment flux from fold and thrust belts. *Basin Res.* 8, 329–349.
- Waibel, A.F., Frisch, W., 1989. The Lower Engadine Window: sediment deposition and accretion in relation to the plate-tectonic evolution of the Eastern Alps. *Tectonophysics* 162, 229–241.
- Wernicke, B., 1981. Low-angle normal faults in the Basin and Range Province: nappe tectonics in an extending orogen. *Nature* 291, 645–648.
- Willet, S., Beaumont, C., Fullsack, P., 1993. Mechanical models for the tectonics of doubly vergent compressional orogens. *Geology* 21, 371–374.
- Winkler-Hermaden, A., 1957. *Geologisches Kräftespiel und Landformung.* Springer, Heidelberg, 822 pp.
- Zweigel, J., Aigner, T., Luterbacher, H.-P., 1998. Eustatic versus tectonic controls on Alpine foreland basin fill: sequence stratigraphy and subsidence analysis in the SE-German Molasse. *Geol. Soc. London Spec. Publ.* 134, 299–323.